DOE Final Report

DOE Award number: DE-SC0019191

Recipient of Award: University of Virginia, University of Virginia, 190 McCormick Rd, Charlottesville, VA 22903

Title: Prediction and Control of Atomic Ordering in Electrodeposited Binary Alloy Films: Direct Synthesis of *L1*0 Magnetic Phases

Principal Investigator: Giovanni Zangari

Period covered in this progress report: 09/01/2018 – 08/31/2021

Submit: June, August, 2023

1. Executive summary

Permanent magnet materials are essential components in renewable energy technology, underlying, electric vehicles, hybrids, wind turbines and more. Today commercial permanent magnets based on Nd-Fe-B exhibit an energy product of ~ 400 kJ/m^3, capable to run wind turbines efficiently. Unfortunately, the supplies of rare-earth elements are centralized, and their availability may see volatility over time. This state of affairs stimulates the search for the search for rare-earth-free permanent magnetic materials. The $L1_0$ crystal structure underlines an important class of chemical ordered alloys that exhibit uniaxial magnetocrystalline anisotropy. This material has been considered an excellent candidate for rare-earth-free permanent magnets.
In this program, a series of systematic experiments were performed and analysed in order to understand the effect of each.
In order to synthesize *L*10-Fe-Ni, one has to circumvent the sluggish kinetic and the limited driving force resulted from the low order-disorder temperature (~320ºC) of the system. A strategy was found to trigger a martensitic transformation from the FCC phase to one of the non-cubic phases by high-strain methods. The body-centered tetragonal Fe-Ni obtained by this strategy was considered as a precursor of *L10* Fe-Ni. The formation of BCT Fe-Ni via a displacive process was also implemented at the nanoscale by using tailored AuNi@FeNi core@shell.

Background: Electrodeposition

The electrodeposition of metals, alloys, and semiconductors utilizes an applied potential or current flowing through an electrolyte solution that contains metal ions. The rate at which a metal deposits is related to the current density by Faraday's law. These metal ions are eventually reduced to atoms at an electrically conducting substrate, thus forming metals or alloys. An alloy is formed by mixing, in solution, mostly, two or more metallic elements in different ratios to enhance the alloy.

Results of the research studied in this program

1. Thin Films of Fe-Ni at Au

The electrodeposition of Fe-Ni alloy is usually complicated by the effects of anomalous co-deposition and hydrogen evolution. Even if the influence of the deposition conditions on the alloy composition has been studied extensively, very few works considered the effect of growth conditions on the phase constitution. Here, we investigate extensively various electrodeposition conditions in a wide range, in order to explore to grow Fe–Ni alloy films (<30 nm) with similar compositions in the Invar-to-equiatomic range on Au (111) substrate. Highly (110) oriented BCC phase Fe–Ni with a Ni fraction (ca. 40 at.% Ni) well beyond the equilibrium solubility limit (5 at.% Ni), possibly inducing different structures. An increase in the fraction of the BCC phase was found, associated with a higher alloy deposition partial current, but not necessarily with an increase in the hydrogen evolution partial current. From this work, we speculate the formation of the metastable BCC phase, depend on the competing kinetics between the inclusion and desorption of hydrogen adatoms at the electrodeposited growth front. According to the Fe–Ni phase diagram, a Ni content of 40 at.% is far beyond the equilibrium solubility limit of Ni (∼5 at.%) in the BCC Fe–Ni, and should also favor the formation of the FCC phase. Despite the formation of BCC Fe–Ni with ca. 40 at.%Ni not being favored by the epitaxial effect of the Au (111) substrate, nor by the supersaturation of the Ni content, pure BCC Fe–Ni with ca. 40 at.%Ni was obtained experimentally from the potentiostatic electrodeposition in this work, specifically from deposition conditions. It is precisely in this sense we suggest that the presence of hydrogen in the electrochemical environment may play a critical role in the formation of the BCC phase Fe–Ni with a composition in the Invar-to-equiatomic range. The relevance of hydrogen in the solute may contribute to the formation of the BCC phase Fe–Ni through different mechanisms, including : (i) surface adsorbed atomic hydrogen (H_{ads}) at the growth front; (ii) through the interstitial hydrogen (H_{ins}), or incorporated into the lattice of the deposited alloy. On the other hand, it was suggested that atomic hydrogen can be incorporated into the lattice in the form of hydrogen interstitial (H_{ins}) during electrodeposition. The presence of H_{ins} in electrodeposited Ni and Fe–Ni ([H]/[M]∼10^{-4}) was demonstrated by Fukai et al. with thermal desorption spect spectroscopy (TDS), suggesting that a significant amount

of lattice vacancies form vacancy-hydrogen clusters with the hydrogen interstitials. The first principle calculation by Zhang et al. indicates that the vacancy formation energy in Ni hydride is lower than that in pure Ni, thus consistent with the suggestion that the presence of hydrogen interstitials contribute to the incorporation of more vacancies. Notice the parallelism between the formation of BCC phase and the incorporation of vacancies: they both evolve towards a more open or less close-packed structure.

On the other hand, it is accepted that the FCC/liquid phase boundary drops to substantially lower temperatures in the presence of hydrogen. In the presence of hydrogen under high pressures, the FCC phase field contracts while the BCC phase field and the liquid phase field expand. Such observations could be extrapolated as another indication that a more open structure is being favored in the presence of hydrogen. Overall, we hypothesize that the formation of highly textured BCC Fe–Ni with a composition ca. 40 at.%Ni on Au (111) substrate found in this work could be explained by the two-fold effect of hydrogen in the electrochemical environment: (1) the presence of surface adsorbed hydrogen (H_{ads}) weakens the bonding between the initially grown Fe–Ni film and the Au substrate, reducing the strain energy associated with the non-pseudomorphic growth of the BCC phase on the FCC (111) surface; (2) the presence of incorporated hydrogen, probably in the form of hydrogen interstitial (H_{ins}), extends the Ni solubility limit in the BCC lattice of Fe–Ni in favor of a more open structure.

Unfortunately, at the cm scale and beyond, we could not detect any different structure.

2. **Anomalous codeposition**

The electrodeposition of metals and alloys may occur through a variety of processes; an important path includes the anomalous co-deposition of alloys. The mechanism of this process derives from the Fe deposition mechanism, described by Bockris, Drazic, and Despic (BDD). The comprehension of this mechanism was developed and refined over time, pushed by the technological importance in electronics. Anomalous codeposition generates a composition gradient zone along the growth direction within the near-substrate region. Even if it has been shown that the composition gradient can be mitigated through the pulsing during growth, a fundamental understanding of this behavior remains unclear. In this work, the evolution of the composition and the morphology during the (pulsed) electrodeposition of Ni-Fe films was reported. The anomalous codeposition of Ni-Fe has a tendence to develop a composition gradient zone within the near-substrate. The composition depth profile along the composition gradient zone was not characterized until more recently by some researches, who studied the influence of the substrate material on the composition gradient zone. Herein, we proposed that the concentration

gradient developed during the initial growth of Ni-Fe codeposition could be explained by the theory described as follows based on the original BDD mechanism. The amount of $Me(OH)^{+}_{ads}$ at the growth front, which was hypothesized to play the key role of a localized pH buffer, could be affected by both the surface coverage and the surface morphology. The pulse-current method could mitigate the composition gradient occurred during the initial growth of Ni-Fe. The impact of the pulse-reverse potential method controls the applied potential instead of the applied current. In this work, we extended the anomalous co-deposition of Ni-Fe on Au (111) substrates beyond the thickness limit of the epitaxial growth, which was indicated by a morphological transition observed with scanning electron microscopy. We also investigated the initial growth of Ni-Fe films grown by the pulse-reverse potential method. The effects of the reverse potential were discussed based on the mechanism of anomalous co-deposition described in the current section.

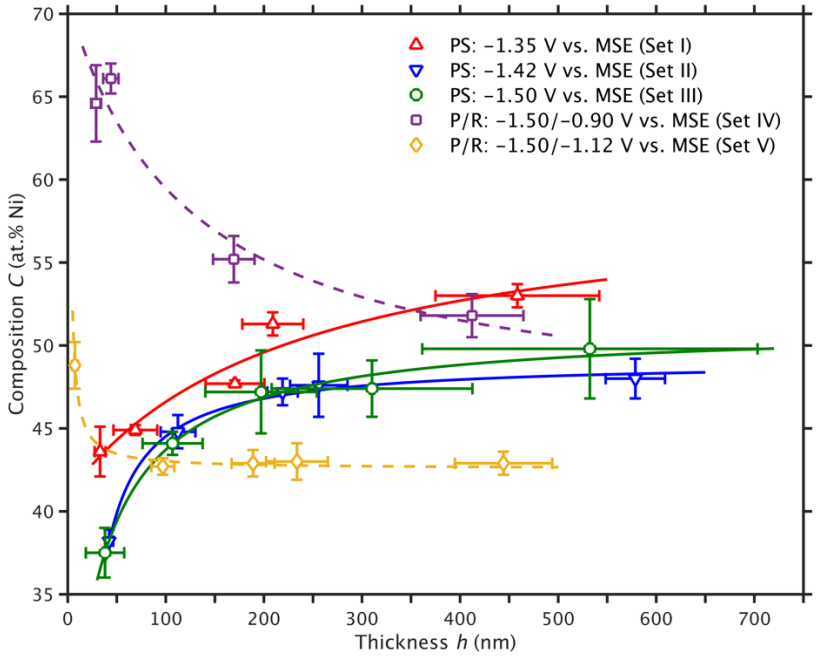

The figure above shows the composition as a function of thickness for each set of films. The films deposited under the potentiostatic mode showed a composition gradient of increasing Ni fraction during the initial growth. The films deposited under the pulse-reverse potential mode, showed a composition gradient of decreasing Ni fraction during the initial growth. Our previous study suggested that the formation of the BCC phase was related to the electrochemical environment at the electrodeposited growth front. The observation described here supports the hypothesis in our previous study.

Based on this mechanism, the composition gradient was a result of the gradual accumulation of Me(OH) + ads at the growth front during the initial growth. The decline of the composition gradient in the subsequent

growth was a consequence of the saturation of Me(OH) + ads at the growth front. In the following, this mechanism was further used to rationalize the pulse-reversed potential deposition behavior. The films grown under the potentiostatic and the pulse-reverse potential mode had opposite composition gradients —an increasing Ni fraction under the potentiostatic mode, as opposed to a decreasing Ni fraction under the pulse- reverse potential mode. This observation strongly suggests that Fe (i.e., the less noble metal) was dealloyed during the initial growth under the reverse cycles. During the subsequent growth, the composition gradient declined under both deposition modes. And the surface morphologies of the films were similar to each other, despite of the difference in the deposition mode and condition. This was in contrast to the drastically dissimilar surface morphologies of the initially grown films. Both the compositional and the morphological behavior suggest that the dealloying process that was present during the initial growth was suppressed during the subsequent growth. The suppression of the dealloying process was rationalized based on the mechanism proposed in the pulse-reverse potential mode, Me(OH) + ads functioned not only as a localized pH buffer, but also as a barrier against dealloying during the reverse cycles. In other words, the Fe atoms covered by Me(OH) + ads at the growth front were less susceptible to being dealloyed. Therefore, as Me(OH) + ads accumulated during the initial growth, the Fe fraction increased, showing the gradient of decreasing Ni fraction. When the growth front was saturated with Me(OH) + ads , the gradient declined, and the composition approached a plateau. Note that Me(OH) + ads was not the only species that adsorbed at the growth front. Boric acid is a buffer that suppresses the pH increase due to hydrogen evolution. In addition to the buffering action, Yin and Lin suggested that boric acid competed with NiOH + and FeOH+ for the adsorption sites, and that the boric acid adsorbed at the growth front selectively blocked the passage and reduction of $NiOH^{+}$,thus augmenting the composition anomaly . Conclusions In this work, we demonstrated the evolution of composition and morphology during the anomalous codeposition of Ni-Fe films. During the initial growth, the potentiostatic mode and the pulse- reverse potential mode both developed a composition gradient, but in opposite signs; during the subsequent growth, the composition gradients under both deposition modes declined, approaching a composition plateau The surface morphologies resulted from the two deposition modes were drastically different during the initial growth, but became increasingly more similar during the subsequent growth In particular, the initial growth under the pulse-reverse potential mode showed morphological features indicative of a dealloying process but the subsequent growth under the same mode did not show such features. The mechanism we proposed in this work, however, accounted for both the composition difference and the composition gradient. The accumulation and the saturation of the adsorbed metal hydroxide ion at the growth front were used to rationalize not only

the occurrence and the decline of the composition gradient under the potentiostatic mode and the pulse-reverse potential mode, but also the opposite signs of the composition gradients under the two deposition modes.

Detecting the absence of cubic symmetry

In this section, we demonstrate the absence of cubic symmetry in near-equiatomic Fe-Ni nanoparticles synthesized by picosecond-pulsed laser ablation in liquids. The non-cubic phase detected in these particles can only be $L1_0$-FeNi or hexagonal close-packed (HCP) FeNi, and the absence of cubic symmetry was unequivocal. The orientation relationship between the non-cubic phase and the adjacent cubic phase was characterized by a series of transmission electron microscopy (TEM) techniques, which consistently suggests that the formation of the non-cubic phase involves a martensitic transformation process. Fe–Ni alloy is usually complicated by the effects of anomalous codeposition and hydrogen evolution. In this work, various electrodeposition conditions were investigated to grow Fe–Ni alloy films (<30 nm) with similar compositions in the Invar range on Au (111) substrate. Highly (110) oriented BCC phase Fe–Ni with a Ni fraction (ca. 40 at.% Ni) well beyond the equilibrium solubility limit (5 at.% Ni) was obtained with a significant alloy deposition partial current. Motivated by the findings from this work, the formation of the metastable BCC phase is speculated to depend on the competing kinetics between the inclusion and desorption of hydrogen adatoms at the electrodeposited growth front.

The identification of L10-FeNi is not a trivial task either. The ordered structure deviates very little from its disorder counterpart, resulting in an which hinders the attempts of using imaging techniques to detect the structure. It is also challenging to resolve the superstructure reflections when using diffraction techniques. So far, for any of the non-cubic Fe-Ni phases, such kind of investigation has not been reported. In this work, we report the structural and morphological characterization of near-equiatomic Fe-Ni nanoparticles prepared by the method of picosecond-pulsed laser ablation in liquids. High- resolution TEM (HRTEM) images of the nanoparticles show the presence of crystallites that do not have the cubic symmetry. The crystal structure of the non-cubic crystallites was identified to be either L10- FeNi or HCP-FeNi. HRTEM imaging and nano-beam electron diffraction (NBED) were used to extract the orientation relationship between the non-cubic phase and the adjacent cubic phase. The results were consistent, and the observed orientation relationship suggests that the formation of the non-cubic phase involves a martensitic transformation process.

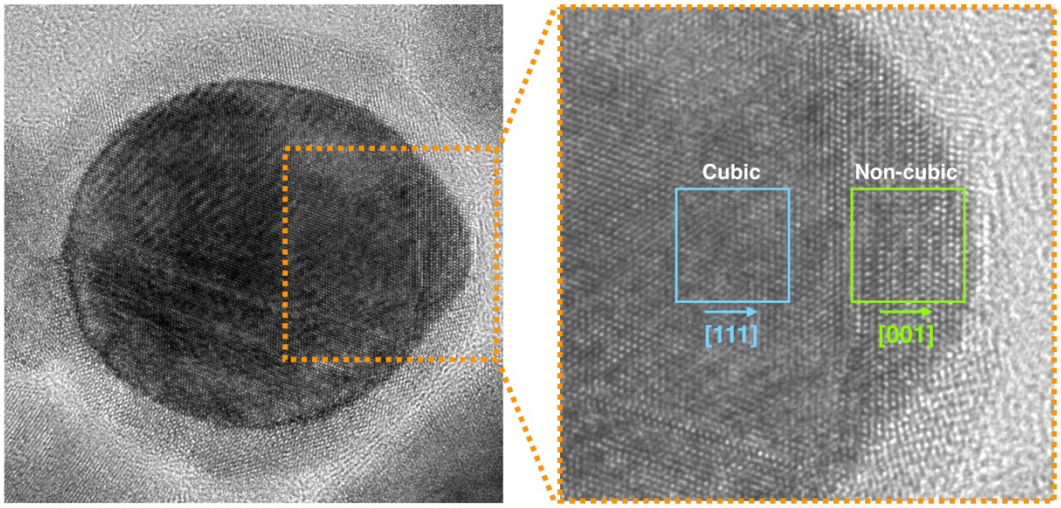

Pulse laser Irradiation

This chapter summarizes the results of a preliminary investigation on the single-pulse laser irradiation of electrodeposited Fe-Ni. The single-pulse laser irradiation changed the grain size as well as the texture of the laser-irradiated site. As the laser fluence was increased, the grain size of laser-irradiated site increased. At the same time, the 111 orientation was suppressed, while the 001 orientation was populated. The 001 direction in L10 Fe-Ni is the unique direction that defines the magnetocrystalline anisotropy, in exactly the sense that a magnetic moment aligned with the 001 direction has the minimum magnetocrystalline anisotropy energy. Developing the 001 texture of FCC Fe-Ni films may aid the detection of the L10 Fe-Ni phase via coercivity measurements.

As it is shown in **Figure 5.9**, the as-deposited site has a 111 PO — the probability of finding a 111 orientation in the as-deposited site is larger than that of finding one in the corresponding reference sample, where each orientation is randomly distributed. The laser-irradiated site of the lowest fluence (F = 0.91 J/m^2) is close to having no PO — the probability of finding a 111 orientation or a 001 orientation is close to that of finding one in the reference sample. As the laser fluence increases, the 001 PO increases monotonically. On the laser-irradiated site of the highest fluence (F = 1.37 J/m^2), the 001 PO is so strong that the 111 PO is significantly smaller than random.

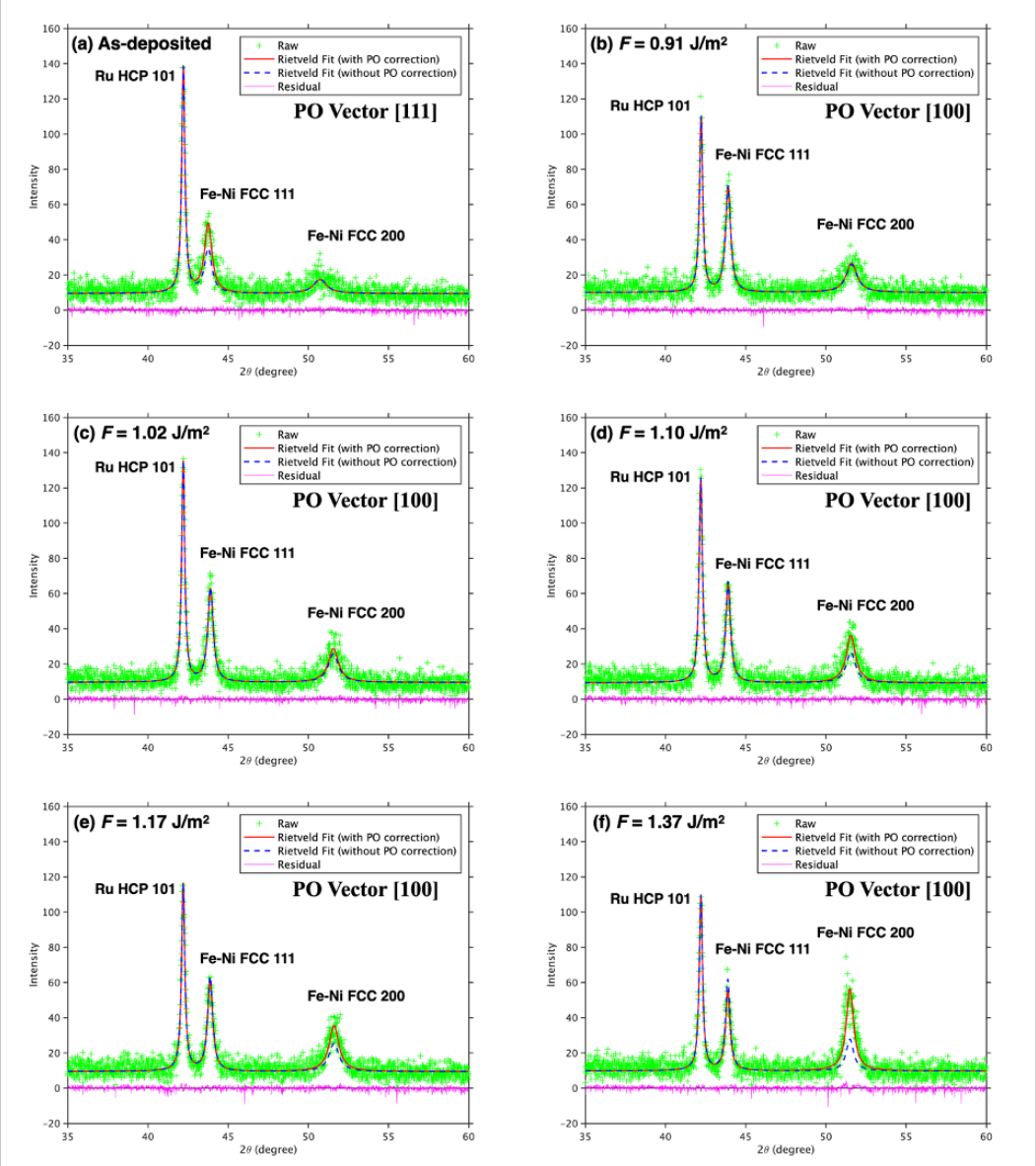

Figure 5.9. Rietveld refinements of experimental XRD patterns with and without the preferred orientation correction. **(a)** As-deposited Fe-Ni. **(b)** Laser-irradiated Fe-Ni (F = 0.91 J/m^2). **(c)** Laser-irradiated Fe-Ni (F = 1.02 J/m^2). **(d)** Laser-irradiated Fe-Ni (F = 1.10 J/m^2). **(e)** Laser-irradiated Fe-Ni (F = 1.17 J/m^2). **(f)** Laser-irradiated Fe-Ni (F = 1.37 J/m^2). The green crosses denote the experimental data. The red solid and blue dashed lines denote the Rietveld fitted pattern with and without the March preferred orientation (PO) correction, respectively. The magenta line shows the residual of the Rietveld fitted pattern with the PO correction.

3. Students and collaborators

The program directly supported the efforts of 1 Ph.D. graduate student, Qiyuan Lin. He successfully his PhD. Dissertation June 24, 2020.

4. Research Products

1) Q. Lin, "Nanoscale Structures in Near-Equiatomic Fe-Ni Films and Particles", PhD Dissertation, 2022.
2) Q. Lin, G. Zangari, "The Evolution of Composition and Morphology during the Initial Growth of Electrodeposited Ni-Fe Films: Comparison between the Potentiostatic Mode and the Pulse-Reverse Potential Mode", *Electrochimica Acta*, 2022, 409: 139978. https://doi.org/10.1016/j.electacta.2022.139978
3) Q. Lin, R. Nadarajah, E. Hoglund, J. M. Howe, B. Gökce, G. Zangari, "Towards Synthetic $L1_0$-FeNi: Detecting the Absence of Cubic Symmetry in Laser-Ablated Fe-Ni Nanoparticles." *Applied Surface Science*, 2021, 150664. https://doi.org/10.1016/j.apsusc.2021.150664
4) Q. Lin, E. Hoglund, G. Zangari, "Electrodeposition of Fe-Ni alloy on Au(111) substrate: Metastable BCC growth via hydrogen evolution and interactions" *Electrochimica Acta*, 2020, 338: 135876. https://doi.org/10.1016/j.electacta.2020.135876
5) S. Ge, Q. Lin (Co-first Author), S. Wodarz, S. Hashimoto, M. Kambe, T. Homma, G. Zangari, "Electrodeposition of Fe-Ni-Pt Alloy Films for Heat-Assisted Magnetic Recording Media: Synthesis, Structure and Magnetic Properties." *Electrochimica Acta*, 2019, 302: 92-101. https://doi.org/10.1016/j.electacta.2019.01.176